ENERGY TRANSFER BETWEEN TWO SITES IN Nd^{3+}:$KLiYF_5$

H. WEIDNER*, P. L. SUMMERS*, R. E. PEALE* AND B. H. T. CHAI**
*University of Central Florida, Department of Physics, Orlando, FL 32816
**University of Central Florida, Center for Research and Education in Optics and Lasers, Orlando, FL 32826

ABSTRACT

High resolution spectroscopy of Nd^{3+} in Potassium Lithium Yttrium Fluoride ($KLiYF_5$) at ≤ 80 K reveals two crystal-field sites which are equally populated independent of concentration. Site selective excitation of photoluminescence distinguishes each site's contribution to the spectra. The analysis of integrated line intensities reveals a bidirectional energy transfer between Nd^{3+} ions in different sites. A rapid increase in transfer rate with increasing Nd concentration is explained only if non-radiative transfer via exchange interaction contributes strongly to the effect. The observed relative decrease with increasing concentration of those emission lines which overlap strongly with opposite-site absorption lines implies that radiative transfer is also important. The energy transfer strongly depends on temperature (2 K - 80 K) which indicates the participation of phonons.

Advances in semiconductor-laser technology have revived the interest in rare-earth activated insulators suitable for diode-pumped lasing. In particular, powerful AlGaAs diode lasers are well suited to pump an absorption band at 0.8 μm for lasing at 1 μm in Nd^{3+} activated materials. Still, considerable improvements over traditional materials such as Nd:YAG are required before practical miniaturized all solid-state 1μm lasers can be realized. In this context, we have grown and studied the new crystal $KLiYF_5$ (KLYF) activated by Nd^{3+} ions. As a laser medium Nd:KLYF was recently reported to have low threshold and high gain.[1,2]

In the course of spectroscopic characterization of our KLYF crystals, new features were revealed that had been missed in previous low resolution studies. Our high resolution spectroscopy reveals, in contradiction to the spectroscopic results of Kaminskii and Khaidukov,[1] that the Nd^{3+} ions occupy two similar sites which have measurably different crystal fields.[3] The two sites are occupied nearly equally by the dopant Nd^{3+} ions. With site selective spectroscopy, we separated the contributions of each site to the spectra and separately determined the energy levels.[3] Here we discovered that the ability to selectively excite luminescence from a single site decreases dramatically with increasing Nd concentration. We will show that energy transfer between sites is responsible for the decreasing selectivity. The technique we used to study the transfer is based on high resolution transmission and photoluminescence spectra obtained in a cw-regime and does not require high spectral- and time-resolution simultaneously. Steady state solutions to simple rate equations are combined with luminescence intensity ratios and independent low resolution fluorescence life time measurements to give transfer rates vs. concentration. These data are then discussed in terms of known energy transfer mechanisms. Repeating the experiments at different temperatures reveals the involvement of phonons in the transfer process.

The crystals were grown by the top-seeded solution growth method with nominal Nd^{3+} concentrations of 0.2%, 2.0%, 3.3%, and 5.0%. The actual Nd^{3+} concentrations (see Table I) in the samples were estimated with the help of the integrated absorption strengths and with the assumption that nominal and actual concentration are equal in the 0.2% sample. The density of

Mat. Res. Soc. Symp. Proc. Vol. 329. ©1994 Materials Research Society

Nd^{3+} ions is then the corresponding fraction of the Yttrium concentration, which is $9.14x10^{21}$ cm^{-3} for undoped crystals.[4] The large optical quality, light violet, monoclinic[5] crystals were oriented for polarized measurements by means of cleavage planes which define the crystallographic b axis.

Both photoluminescence and absorption spectra were taken with a Bomem DA8 Fourier transform spectrometer. The detector was a silicon photodiode, the beamsplitter quartz, and the source for transmittance a quartz-halogen lamp. A jet-dye laser (dye: DCM) pumped by a multi-line Argon-ion laser was used for site selective excitation of photoluminescence. The laser frequency was selected with a birefringent plate ($\Delta\upsilon = \pm 3$ cm^{-1}) calibrated by directly measuring the laser output with the Fourier spectrometer. The FWHM of the laser output was ≤ 2 cm^{-1}. The width of the beam was slightly larger than the sample (~ 10 mm) which allowed, together with weak absorption, for a uniform excitation within the sample volume. Measurements at 80 K made use of a home-made liquid-nitrogen cold-finger cryostat. Measurements below 80 K were performed with a Janis supervaritemp liquid-helium cryostat.

Table I. Nominal and actual concentrations, fluorescence life times and inverse intersite transfer rates for Nd^{3+}:$KLYF_5$ at 80 K.

concentration (%) nominal	actual	fluorescence life time (μs)	(transfer rate)$^{-1}$ (μs)
0.2	0.2	521	2110
2.0	1.28	482	118
3.3	1.65	411	62
5.0	1.99	349	24

For fluorescence lifetime measurements, the samples were excited with filtered light (13000 to 23000 cm^{-1}) from a flash lamp giving pulses of 30 μs duration with a repetition rate of about 2 Hz. The sample emission passed a low-pass filter (≤ 12800 cm^{-1}), was detected with a silicon detector, and was digitally recorded as a function of time with a time resolution of 13 μs. The decays were adequately described by a single exponential function, which indicates that the decay rates of both sites are approximately equal. The 1/e decay times given in Table I decrease with increasing concentration but vary only slightly with temperature.[2] Since the emission from the $^4F_{3/2}$ levels dominates in the detected range, the obtained decay times represent the lifetimes of the $^4F_{3/2}$ manifold of Nd^{3+} in the different samples.

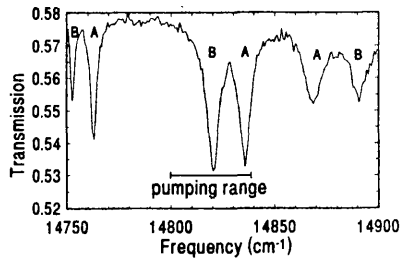

Figure 1. Portion of the Nd^{3+}:KLYF $^4I_{9/2}$ → $^4F_{9/2}$ transmission spectrum. The nominal concentration was 2%. The sample temperature was 80 K. The letters assign transitions to sites.

Fig. 1 presents a part of the $^4I_{9/2}$ → $^4F_{9/2}$ transmission spectrum at 80 K. These transitions are used to absorb the dye-laser excitation. The spectrum was taken with the 2% sample, but positions, widths and relative strengths of the lines are nearly identical for all concentrations studied. The laser excitation in the studies to be discussed below was varied over the range indicated in Fig. 1. This range contains one transition from the ground state of each site and none from thermally populated Stark levels of the ground term. Therefore, one expects site B photoluminescence to be the strongest when the laser is tuned to the center frequency of the B line at 14820 cm^{-1}. Moreover, site B photoluminescence intensity should decrease monotonically when the laser frequency is shifted away from the B absorption peak. Specifically, site B emission should not

increase again when the laser is tuned through the site A absorption line. However, Fig. 2 reveals that a different behavior becomes obvious in the higher concentration samples. It shows a portion of the 2% sample's $^4F_{3/2} \rightarrow {}^4I_{11/2}$ emission for the pump range marked in Fig. 1. Each site's emission line peaks twice as the excitation is tuned through the absorption line pair. In other words, site A (B) emission reaches a maximum when either site A or site B is resonantly excited. Hence, the two sites must be coupled by energy transfer, and this transfer can occur in both directions (A→B and B→A).

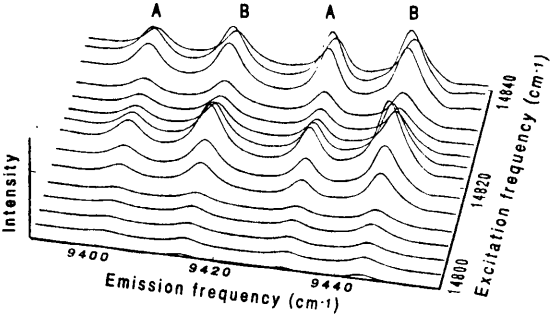

Figure 2. Portion of the Nd^{3+}:KLYF $^4F_{3/2} \rightarrow {}^4I_{11/2}$ luminescence spectra at 80 K for a series of excitation frequencies. The nominal concentration was 2%.

To quantify the energy-transfer effect, ratios of integrated line strengths were determined. These ratios were taken between members of emission-line pairs with one line from each site, i.e. $(I_A \cdot \Delta\nu_A)/(I_B \cdot \Delta\nu_B)$. The line heights I_A and I_B as well as the line widths $\Delta\nu_A$ and $\Delta\nu_B$ were obtained from nonlinear least squares fits of Voigtian lines to the photoluminescence spectra. In these ratios, uncertainties in the total intensity due to fluctuations in laser power or alignment are divided out. This method of analysis has been widely used in energy transfer studies.[5,6] A comparison of intensity ratios vs. excitation frequency for the four different concentrations at 80 K is shown in Fig. 3. The symbols represent the ratios obtained from the spectra whereas the lines are theoretical fits using the model presented below. The 3 cm^{-1} uncertainty in excitation frequency is sufficient to explain the discrepancies between points and curves. The maximum error of the intensity ratios was estimated to be 5%. All curves have their minimum value near the maximum absorption of site B (largest I_B) and a maximum near the absorption peak of site A (largest I_A). The difference between maxima and minima decreases with increasing concentration. Evidently, energy transfer increases with concentration and tends to equilibrate the emission from both sites regardless of which site is resonantly excited by the laser. Another feature of the intensity ratios is remarkable: The maxima and minima lie symmetrically about a ratio not quite equal to unity. The point of symmetry varies for different (A,B) transition pairs. All curves for a given Nd^{3+} concentration are parallel but shifted, which means that ratios for different (A,B) pairs differ by a constant factor. Both the concentration dependence of the maxima-minima difference and the shift will be explained by our model.

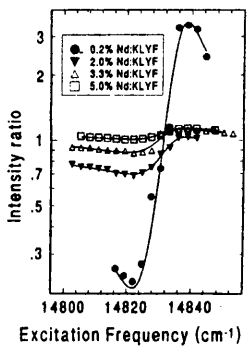

Figure 3. Intensity ratios I_A/I_B of the 9536 cm^{-1} and 9545 cm^{-1} emission lines vs. excitation frequency. (symbols = experiment; curves = fits according to our model).

Evidence for the occurrence of radiative energy transfer is shown in Fig. 4. It shows for the 2% sample the $^4I_{9/2} \rightarrow {}^4F_{3/2}$ transmission spectrum, which is representative for all concentrations. Also shown are $^4F_{3/2} \rightarrow {}^4I_{9/2}$ emission spectra for the 0.2% and 2% samples with the same excitation frequency. The 2% emission was scaled by a constant factor to match the 0.2% sample's emission intensity. Small differences are possible due to changes in branching ratios. However, the lines at and above

11500 cm^{-1} show a rather remarkable decrease with increasing concentration. Since these four transitions (two of which accidentally coincide) from the $^4F_{3/2}$ manifolds to the ground states of the two sites coincide with the respective absorption lines, the observed decrease is likely caused by reabsorption, which allows energy transfer to occur. In particular, the two coincident transitions at 11500 cm^{-1} (one from each site) overlap completely with the corresponding absorption from both sites, which strongly suggests that sites A and B are coupled by radiative transfer. But since the $^4F_{3/2} \rightarrow {}^4I_{9/2}$ emission is significantly weaker than the $^4F_{3/2} \rightarrow {}^4I_{11/2}$ emission, the radiative transfer rate must be significantly less than the radiative decay rate. However, the strong spectral overlap observed implies that resonant *non-radiative* transfer may also be important.

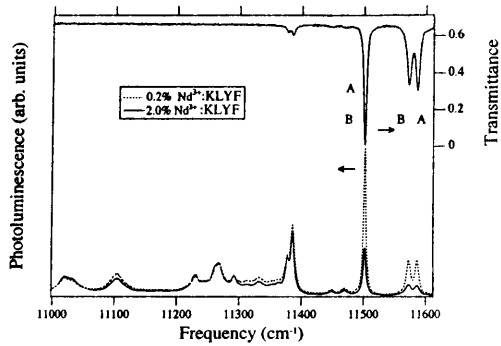

Figure 4. Nd^{3+} transmission (2% sample) and emission spectra (0.2%, 2%) for the $^4I_{9/2} \leftrightarrow {}^4F_{3/2}$ transitions at 80 K. The 2% emission was scaled to match that of the 0.2% sample.

Fig. 5 shows schematically the energy-level diagrams for the two sites and the important transitions. B_A and B_B are the Einstein coefficients for the absorption process in site A and B, respectively. From the $^4F_{9/2}$ manifold, the ions relax rapidly and non-radiatively to the $^4F_{3/2}$ manifold. A_A and A_B are the Einstein coefficients for the total decay rates of the $^4F_{3/2}$ levels. The C_B and C_A are concentration dependent transfer rates towards site B and A, respectively. Using these coefficients one obtains the following rate equations:[5,6,7]

$$dn_A/dt = -A_A\, n_A + B_A\, u\, N_A - C_B\, n_A + C_A\, n_B \qquad (1)$$

$$dn_B/dt = -A_B\, n_B + B_B\, u\, N_B - C_A\, n_B + C_B\, n_A \qquad (2)$$

where the N_i are the numbers of Nd^{3+} ions per unit volume in site i, and n_i the number of these per unit volume in excited $^4F_{3/2}$ states. The energy density of the pump light is u. The assumption $n_i \ll N_i$ was made (no stimulated emission, no depletion of the ground state). This is reasonable for the pump power used of <100 mW distributed over a sample volume of >0.1 cm^3. In such a low-power regime, each excitation can be treated as spatially and temporally isolated and behaves according to the probabilities for its decay, diffusion, and transfer. Therefore, the n_i are proportional to the pump intensity, and hence the intensity ratios of the emission and the transfer rates are independent of pump power.

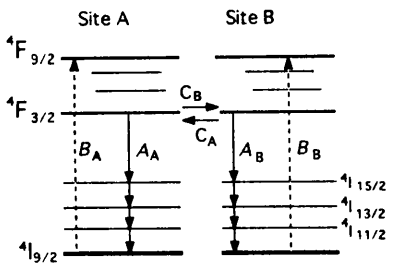

Figure 5. Schematic level diagram for Nd^{3+} in each site and important transition rates. A_i = spontaneous decay; B_i = absorption; C_i = transfer into site i.

Assuming that the laser line is much more narrow than the absorption line, B_i u can be replaced by α_i/N_i times the photon flux density of the pump source. Here α_i is the site i absorption coefficient obtained from transmission spectra. Further simplifications

follow from the similarities of the two sites ($A_A=A_B=A$, $C_A=C_B=C$). Steady state solutions ($dn_i/dt = 0$) give the n_i and the emission intensities $I_{ij} = b_{ij} n_i$. Index i distinguishes the two sites and index j numbers individual transitions. The proportionality factor b_{ij} includes the oscillator strength of the j^{th} transition at site i, the energy of the emitted photon and the experimental response function. Only the n_i are effected by tuning the excitation. Connection to the experiment is made by taking the ratio:

$$I_{Aj}/I_{Bj} = (b_{Aj}/b_{Bj}) \cdot \frac{(\alpha_A + \alpha_B) \cdot C/A + \alpha_A}{(\alpha_A + \alpha_B) \cdot C/A + \alpha_B} \quad . \tag{3}$$

Adjusting the two free parameters in Eq. 3 (b_{Aj}/b_{Bj} and C/A) to fit the experimental intensity ratios leads to the curves in Fig. 3. The vertical shifting observed for the actual data is achieved by varying b_{Aj}/b_{Bj}, indicating that relative oscillator strengths for the two sites differ from transition to transition. Since b_{Aj}/b_{Bj} is always close to unity, the difference is slight. This is confirmed in absorption spectra because lines belonging to a pair are always about equally strong (see Figs. 1, 4 and Ref. [3]). Varying C/A in Eq. 3 changes the difference between maximum and minimum: Increasing C/A makes the intensity ratio more nearly equal to b_{Aj}/b_{Bj} and independent of excitation frequency. The observed decrease in the variation of the intensity ratio with increasing concentration (Fig. 3) is therefore explained by an increase in C/A. With A (the inverse of the fluorescence life time) and the fits of Eq. 3 to our data, we obtain the transfer rate C for each concentration. The 80 K transfer times (1/C) for our samples are given in Table I.

Fig. 6 presents the concentration dependence of C for 2 K and 80 K. The experimental results are represented by the points. The curves are approximations according to different microscopic models of energy transfer[8-11] assuming a homogeneous density N of Nd^{3+} ions in the crystal. Curves b (dotted line) and a (dashed line) assume quadrupole-quadrupole ($C \sim N^{10/3}$) and dipole-dipole ($C \sim N^2$) interactions, respectively. As seen in Fig. 6, even an exponent of 10/3 is insufficient to describe the steep increase of the energy transfer rate C. Higher exponents can be obtained from higher multipole interactions, but these are unlikely because of the rapidly decreasing strength of such interactions. Radiative transfer has a concentration dependence[9] of only $a_2 N^{2/3}$ and would, if added to a transfer via multipole interaction, require even higher exponents for the latter. (Super-) Exchange interaction, on the other hand, has a concentration dependence of $a_1 \cdot \exp(-N^{-1/3}/L)$, with $N^{-1/3}$ being a measure for the distance between interacting Nd^{3+} ions and L a constant of the order of the characteristic interaction length.[8,11] The exponential dependence taken alone allows for a steep increase at high concentrations but severely underestimates the transfer rate for the 0.2% sample. Therefore we include also radiative transfer, and a sum of the two mechanisms is plotted as curve c (solid line) for both 80 K and 2 K. The parameters giving these fits are listed in Tab. II. The value determined for L has the expected order of magnitude.[10,11] The necessity of exchange interaction to explain the steep increase of the transfer rate does not exclude the simultaneous existence of transfer via multipole interactions. However, the number of different concentrations presently available is insufficient to determine

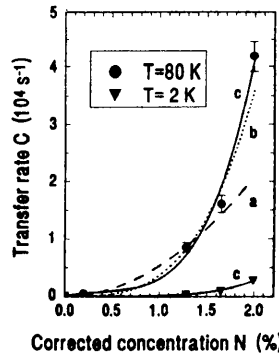

Figure 6. Concentration dependence of the intersite transfer rate for Nd^{3+}:KLYF at 2 K and 80 K. Curves are fits: a: $C \sim N^2$; b: $C \sim N^{10/3}$; c: $C = a_1 \exp(-N^{-1/3}/L) + a_2 \cdot N^{2/3}$

Table II. Fitting parameters for transfer rate vs. concentration $C=a_1 \exp(-N^{-1/3}/L) + a_2 N^{2/3}$

Temperature	a_1 (s^{-1})	L (Å)	a_2 (m^2/s)
80 K	3.5×10^{10}	1.3	7.4×10^{-15}
2 K	2.3×10^{9}	1.3	1×10^{-16}

the relative contribution of each possible process. In addition, intrasite transfer (diffusion) may cause the relative contributions of each mechanism to vary with concentration. In giving concentration independent a_1 and a_2, we have assumed this effect to be negligible.

Fig. 7 shows the temperature dependence of the fitting parameter C/A for the two highest concentrations. After a rapid increase below 30 K, C/A drops at 80 K to less than half of the maximum value. Additional temperature dependent measurements are being performed to clarify this unusual effect.

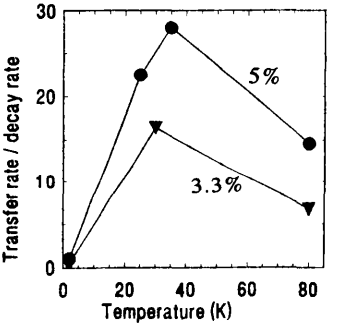

Figure 7. Temperature dependence of the ratio of transfer and decay rates (C/A) for the two highest concentration samples.

To summarize, we have shown that Nd^{3+} dopant ions in the two different crystal-field sites of KLYF exchange energy via bidirectional transfer. The transfer rate increases rapidly with increasing Nd^{3+} concentration and varies strongly in the range from 2 K to 80 K. Both non-radiative transfer via the (super) exchange interaction and radiative transfer appear to contribute significantly. We view Nd:KLYF as a model system for studying energy transfer in multisite crystals. The use of high resolution Fourier spectroscopy, cw site-selective excitation, and a concentration series to study energy transfer is in principle applicable also to a wide range of other materials.

1. A. A. Kaminskii and N. M. Khaidukov, Phys. Stat. Sol. (a) **129**, K65 (1992).
2. J. F. H. Nicholls, X. X. Zhang, G. D. Loutts, B. Henderson, M. Bass, and B. H. T. Chai, in Growth, Characterization, and Applications of Laser Host and Non-linear Crystals II, edited by B. H. T. Chai (SPIE Proc. **13**, 1993) p. 1863.
3. H. Weidner, P. L. Summers, R. E. Peale, and B. H. T. Chai, accepted J. Appl. Phys.
4. A. V. Goryunov, A. I. Popov, and N. M. Khajdukov, Mat. Res. Bull. **27**, 213 (1992).
5. L. D. Merkle and R. C. Powell, Phys. Rev. B **20**, 75 (1979).
6. M. Zokai, R. C. Powell, G. F. Imbusch, and B. Di Bartolo, J. Appl. Phys. **50**, 5930 (1979).
7. J. K. Tyminski, C. M. Lawson, and R. C. Powell, J. Chem. Phys. **77**, 4318 (1982).
8. D. L. Dexter, J. Chem. Phys. **21**, 836 (1953).
9. G. Boulon, in Energy Transfer Processes in Condensed Matter, edited by B. Di Bartolo (Plenum, New York, 1984), p. 603.
10. B. Henderson and G. F. Imbusch, Optical Spectroscopy of Inorganic Solids, (Clarendon, Oxford, 1989), p. 445.
11. B. Di Bartolo, in Energy Transfer Processes in Condensed Matter, edited by B. Di Bartolo (Plenum, New York, 1984), p. 103.